Dynamic Optimization of an Industrial Semi-batch Nylon 6 Reactor with End Point Constraints and Stopping Conditions

NAVEEN K. KOHLI, RAJEEV SAREEN, and SANTOSH K. GUPTA*

Department of Chemical Engineering, Indian Institute of Technology, Kanpur 208 016, India

SYNOPSIS

In this study, optimal vapor release rate (or pressure) histories have been generated for an industrial semi-batch nylon 6 reactor using Pontryagin's minimum principle. The batch time has been taken as the objective function, which is to be minimized. The pressure is constrained to lie between a lower and an upper limit. The temperature, a state variable, is also constrained to lie between 220°C and 270°C in order to ensure single-phase polymerization. Optimization has been carried out with a single end-point constraint (on monomer conversion) and a stopping condition (obtaining a product having a desired degree of polymerization, μ_n). Techniques have been developed to overcome the discontinuities present in the model, as well as to take care of state variable constraints. The effects of various physical and computational variables on the optimal pressure history and the corresponding batch time have been studied. It is found that the optimal batch time is almost 50% of the industrial value used currently. Interestingly, the optimal pressure history is quite similar *qualitatively* with the current practice though *quantitatively* there is a significant difference. Improvements in reactor operation along these lines have been reported. © 1996 John Wiley & Sons, Inc.

INTRODUCTION

A significant amount of research on the simulation of nylon 6 polymerization has been reported in the past few years. These have formed the subject of several reviews.[1-5] The effects of various operating variables (initial water concentration, temperature, monofunctional acid stabilizers, initial monomer concentration, etc.) on the characteristics of the product [viz., monomer conversion, degree of polymerization (DP or μ_n), polydispersity index (PDI), etc.] are now well established. The early reports have been followed by several studies[6-16] on the optimization of nylon 6 reactors. Hoftyzer and coworkers[6] used dynamic programming to determine the optimal temperature and water concentration (related to total applied pressure) histories, $T(t)$ and $[W](t)$, required for producing nylon 6 having a desired value, $\mu_{n,d}$, of the degree of polymerization in the shortest possible reaction time, t_f. Unfortunately, Hoftyzer and colleagues presented only semiquantitative results, because of proprietary reasons. Reimschuessel and Nagasubramanian[7,8] optimized combinations of two-stage isothermal reactors, and presented quantitative results. These two studies made use of a kinetic scheme involving only the major reactions (ring opening, polycondensation, and polyaddition). Naudin ten Cate[9] and Mochizuki and Ito[10] used the minimum principle to find optimal temperature profiles in tubular reactors. Naudin ten Cate optimized a two-stage reactor, the first one at temperature T_0, having a residence time t_0, in which water is vaporized continuously. This was followed by a nonvaporizing tubular reactor having a residence time $t_f - t_0$. Mochizuki and Ito, however, optimized a single reactor. Both these groups of workers used semiempirical approximations for the rates of formation of the undesirable cyclic oligomers, and attempted to minimize the formation of the water extractible compounds (cyclic oligomers, water, and unreacted monomer) while simultaneously keeping some product characteristics fixed (end-point constraints). These workers assumed no evaporation of water and/or caprolactam and obtained optimal

* To whom correspondence should be addressed.

Journal of Applied Polymer Science, Vol. 62, 1219–1230 (1996)
 CCC 0021-8995/96/081219-12

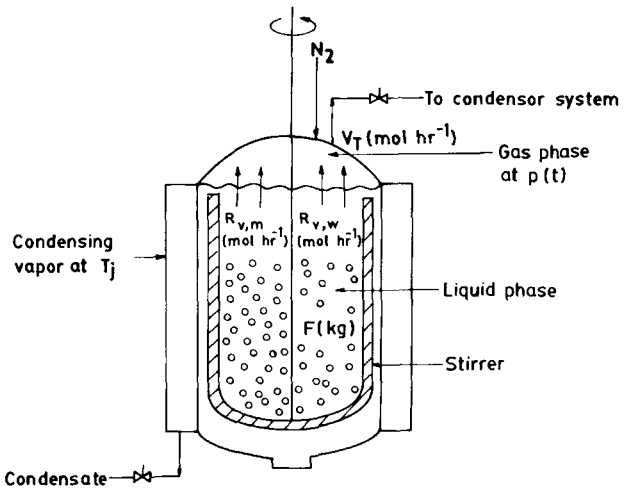

Figure 1 Schematic representation of the industrial semi-batch nylon 6 reactor.

temperature histories. Again, only semiquantitative results were presented. Dynamic optimization of batch (or tubular) reactors using a variety of objective functions and end-point constraints has been carried out by our group[11-16] using Pontryagin's minimum principle.[17,18] These studies have shown that the optimal histories are largely dependent, both qualitatively and quantitatively, on the choice of the objective function and the constraints. This observation is consistent with similar observations made by Ray and Szekely[17] and Denn,[18] who have compiled the results of several optimization studies for nonpolymeric systems. Most of these studies give valuable insight into the optimal operation of *ideal* reactors, and indeed, these must have been used in the design and improvement of nylon 6 reactors in industry over the years. Work on the modeling of actual *industrial* reactors has only just started to appear in the open literature.[19] In this paper, the operation of one such reactor (semi-batch nylon 6 reactor) has been optimized using Pontryagin's minimum principle.[17,18,20,21] Optimal pressure histories have been obtained for the manufacture of three grades of polymer. Substantial improvements are possible in the performance of this reactor once these are implemented.

The industrial reactor studied here is shown schematically in Figure 1. It is a jacketed vessel with a low-speed anchor or ribbon agitator used for mixing the highly viscous reaction mass. The reaction mass is heated by condensing vapors in a jacket. The pressure inside the reactor, $p(t)$, is maintained to conform to a desired history by manipulation of a control valve which allows the vapor mixture of nitrogen, monomer, and water to pass to a condenser. The pressure histories used currently (referred to as "reference" conditions) for three different industrial runs producing different grades of nylon 6, are shown in Figure 2 (curves marked "ref"). In this figure, the pressure and the reaction time, t, have been nondimensionalized according to Wajge and colleagues[19] (see Nomenclature):

$$\Pi \equiv (p - p_0)/(p_{\max,\text{ref}} - p_0) \tag{1}$$

$$\tau \equiv t/t_{f,\text{ref}} \tag{2}$$

The values of the maximum pressure, $p_{\max,\text{ref}}$, and the total reaction time, $t_{f,\text{ref}}$, used currently, are not being reported for proprietary reasons. The jacket temperature, T_j, is kept constant throughout the reaction at the current value, $T_{j,\text{ref}}$.

FORMULATION

The kinetic scheme for nylon 6 polymerization is given in Table I.[4] This kinetic scheme incorporates the three important reactions, ring opening, polycondensation, and polyaddition, as well as reactions with the cyclic dimer. Because of the unavailability of precise information about the rates of the reactions involving higher cyclic oligomers, these have not been incorporated into Table I. Since the cyclic dimer constitutes a major share of the total cyclic

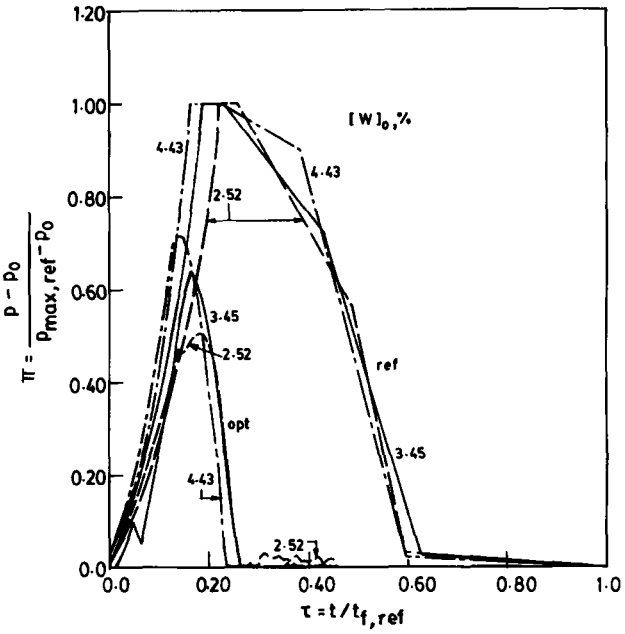

Figure 2 Dimensionless pressure (Π) histories for the reference (ref) and optimal (opt) runs, for $T_j = T_{j,\text{ref}}$, $[W]_0$ = 2.52%, 3.45%, 4.43%.

Table I Kinetic Scheme for Nylon 6 Polymerization

1. Ring Opening $C_1 + W \underset{k_1' = \frac{k_1}{K_1}}{\overset{k_1}{\rightleftharpoons}} S_1$

2. Polycondensation $S_n + S_m \underset{k_2' = \frac{k_2}{K_2}}{\overset{k_2}{\rightleftharpoons}} S_{m+n} + W$; $n, m = 1, 2, \cdots$

3. Polyaddition $S_n + C_1 \underset{k_3' = \frac{k_3}{K_3}}{\overset{k_3}{\rightleftharpoons}} S_{n+1}$; $n = 1, 2, \cdots$

4. Ring Opening of Cyclic Dimer $C_2 + W \underset{k_4' = \frac{k_4}{K_4}}{\overset{k_4}{\rightleftharpoons}} S_2$

5. Polyaddition of Cyclic Dimer $S_n + C_2 \underset{k_5' = \frac{k_5}{K_5}}{\overset{k_5}{\rightleftharpoons}} S_{n+2}$; $n = 1, 2, \cdots$

Rate and Equilibrium Constants

$$k_i = A_i^0 exp(-E_i^0/RT) + A_i^c exp(-E_i^c/RT) \sum_{n=1}^{\infty} ([S_n])$$

$$= k_i^0 + k_i^c \sum_{n=1}^{\infty} ([S_n])$$

$$K_i = exp[(\Delta S_i - \Delta H_i/T)/R], \; i = 1, 2, \cdots, 5$$

i	A_i^0 (kg mol^{-1} h^{-1})	E_i^0 (J mol^{-1})	A_i^c (kg^2 mol^{-2} h^{-1})	E_i^c (J mol^{-1})	ΔH_i (J mol^{-1})	ΔS_i (J mol^{-1} K^{-1})
1	5.9874×10^5	8.3198×10^4	4.3075×10^7	7.8703×10^4	$+8.0268 \times 10^3$	-32.9970
2	1.8942×10^{10}	9.7389×10^4	1.2114×10^{10}	8.6504×10^4	-2.4883×10^4	$+3.9496$
3	2.8558×10^9	9.5606×10^4	1.6377×10^{10}	8.4148×10^4	-1.6923×10^4	-29.0680
4	8.5778×10^{11}	1.7577×10^5	2.3307×10^{12}	1.5652×10^5	-4.0176×10^4	-60.7660
5	2.5701×10^8	8.9141×10^4	3.0110×10^9	8.5374×10^4	-1.3263×10^4	$+2.4384$

oligomers in the reaction mass, this assumption is justified. The rate constants as well as the equations for the 15 state variables, x_i (mass and energy balance, and moment equations) are given by Wajge and coworkers[19] and are not repeated here for the sake of brevity. In general, the state variable equations can be expressed as

$$\frac{dx_i}{dt} = f_i(\boldsymbol{x}, \boldsymbol{u}); \; i = 1, 2, \ldots, 15 \qquad (3)$$

where $\boldsymbol{x}$ and $\boldsymbol{u}$ are the vectors of the state and control variables.

The ordinary differential equations (ODEs) in eq. (3) can be integrated using the D02EJF subroutine of the NAG library. This uses Gear's technique for integrating sets of stiff ODEs.[22] The presence of some discontinuities and the stiffness of ODEs make it difficult to use a constant error tolerance (TOL) in the computer code. Provision was made in the algorithm for self-adjustment of the error tolerance between 10^{-4} and 10^{-12}. When D02EJF failed to solve the ODEs with the given error tolerance, it came out of the subroutine giving an error message, IFAIL = 2. At this point a backward step was taken and TOL reduced by a factor of 10. The ODEs were again integrated in the forward direction. This backward movement was continued with a reduction in TOL, and the integration repeated until the solution was obtained. A similar procedure was followed for the backward integration of the adjoint variables. The change in viscosity of the reaction mixture and its effect on the mass transfer rates have been incorporated[19] using correlations for the

viscosity of the reaction mass and the activity coefficients of water and caprolactam. These correlations have been developed[19] by curve-fitting one set of industrial data, and have been found to be satisfactory for other operating conditions.

The simulation package can be used to predict several important properties of the product (μ_n, PDI, monomer concentration, cyclic dimer concentration, etc.) as well as the various reactor characteristics [heat and mass transfer coefficient, vapor discharge rate, $V_T(t)$, temperature, etc.]. The model of the industrial semi-batch nylon 6 reactor can be used to optimize its operation. In this study, we obtain the optimal vapor-release-rate history, $V_T(t)$, which minimizes the total reaction time, t_f, while requiring a few constraints to be met at $t = t_f$. The objective function, I, to be minimized is selected as the dimensionless total reaction time:

$$\min I[\boldsymbol{x}(t), t_f] \equiv t_f/t_{f,\text{ref}} \tag{4}$$

where $t_{f,\text{ref}}$ is the total reaction time being used in the reference case (current value). We choose the following constraint at the end point:

$$\psi_1 \equiv conv_{t_f} - conv_d = 0 \tag{5}$$

where the monomer conversion, *conv*, at the end of the reaction is forced to be equal to a desired value, $conv_d$, selected as the current value. This ensures no additional load on downstream extraction units. In addition, we use the following stopping condition:

$$\rho \equiv \mu_{n,t_f} - \mu_{n,d} = 0 \tag{6}$$

where the number average chain length of the product, μ_{n,t_f}, is forced to be equal to a desired (current) value, $\mu_{n,d}$. In eqs. (4)-(6), we have (see Nomenclature):

$$conv = 1 - \frac{F[C_1] + \zeta_1}{F_0[C_1]_0} \tag{7}$$

$$\mu_n = \mu_1/\mu_0 \tag{8}$$

The stopping condition on μ_n ensures the required quality and physical properties of the product (the stopping condition and the end-point constraints are interchangeable—in fact, if there are several requirements at $t = t_f$, any one can be selected as the stopping condition).

The problem defined in eqs. (4)-(6) involves three important characteristics of nylon 6 reactors: monomer conversion, μ_n, and reaction time. One would also like to minimize the cyclic dimer concentration, $[C_2]_{t_f}$ in the product, *simultaneously*. This, however, would lead to a dynamic multiobjective optimization problem, involving the generation of a Pareto set.[16,23] Such a problem is associated with severe computational problems for the semibatch reactor studied here, and one must have a good knowledge of solutions of simpler optimization problems before one can hope to solve for the Pareto sets. It is hoped that the simpler problem defined in eqs. (4)-(6) will lead to sufficiently low values of $[C_2]_{t_f}$ (compared to values encountered currently) and will be satisfactory as well as useful for industrial implementation.

The algorithm for the *general* optimization problem (with one stopping and m end-point constraints as well as n state variable equations and l control variables) is given by Ray and Gupta.[14] In the present case, three sets of adjoint variables, λ_i^I, $\lambda_i^{\psi_1}$, and λ_i^{ρ} ($i = 1, 2, \ldots, n$) have to be evaluated. The ODEs defining these variables are similar in form but their values differ because of the different boundary conditions at $t = t_f$. The numerical procedure used is as follows[14]:

1. An initial control variable history (a single control variable, $u \equiv V_T$, is used in this study), $V_T^0(t)$, is selected. In order to reduce the memory storage requirements, the values of V_T^0, and the λ's are stored at intervals of 0.1 h and linear interpolation is used. The 15 state variable equations with known initial values, $\boldsymbol{x}(0)$, are then integrated in the forward direction using the D02EJF subroutine of the NAG library. The forward integration is carried out until the stopping condition of eq. (6) is satisfied within some tolerance limit (10^{-2} in this study). This fixes the value of t_f. During the forward integration, the values of $\partial \boldsymbol{f}/\partial V_T$ and $\partial \boldsymbol{f}/\partial \boldsymbol{x}$[14] are also computed (numerically) and stored at time intervals of 0.1 h.
2. The adjoint variable equations are then integrated in the backward direction until $t = 0$, using the D02EJF subroutine, and the boundary conditions at $t = t_f$. The modified adjoint variables, $\lambda_i^{I\rho}(t)$ and $\lambda_i^{\psi_1\rho}(t)$, are computed at each storage location ($\Delta t = 0.1$ h). In addition, the three integrals, $I_{\psi_1\psi_1}$, $I_{\psi_1 I}$, and I_{II}, are computed using the D01GAF subroutine of the NAG library.
3. Values of two computational parameters, r and ϵ^*,[14] are selected, and the correction, δV_T,

computed at each storage location. The new vapor-release-rate history, V_T^{new}, is generated using:

$$V_T^{new}(t) = V_T^0(t) + \delta V_T(t) \qquad (9)$$

4. This completes one iteration. These steps may be repeated (using the new V_T history as V_T^0) until there is no change in the pressure (or V_T) history and the end-point constraints are satisfied to a prescribed degree of accuracy (because first-order techniques converge very slowly as the optimum is reached).

While carrying out the optimization, it was desired to constrain some of the state variables to lie between lower and upper bounds:

$$0 \leq \Pi \leq 1.0 \qquad (10)$$

$$220°C \leq T \leq 270°C \qquad (11)$$

The upper bound on pressure does not allow the pressure rating of the industrial reactor to be exceeded while the lower bound ensures the pressure inside to be above atmospheric. The lower limit on T is the melting point of nylon 6 whereas the upper limit represents the approximate boiling point of pure caprolactam (at atmospheric pressures). A standard procedure of satisfying these constraints on the state variables is to incorporate them into the objective function as penalty functions. Our previous experience (initial runs) has shown that the temperature in the reactor almost never violates the constraints. Therefore, the only state variable for which constraints need to be taken care of is the pressure inside the reactor. This is controlled by the vapor discharge rate, V_T, from the reactor. This suggests an empirical (and easier) approach to satisfy the constraints on $p(t)$ in eq. (10). Some conditional statements have been included in the computer code, which take care of the pressure going below or above the lower and upper values, respectively. Whenever the pressure drops below p_0, V_T is decreased in infinitesimally small steps till the lower bound is satisfied. In a similar way, the upper bound in eq. (10) is taken care of. The computer code so developed was found to work satisfactorily. The correctness of the code was checked by running it for some special cases. The program was run in the simulation mode, using $V_T(t)$ from Wajge and coworkers.[19] The results were in complete agreement with the earlier simulation results, thereby suggesting that at least in the simulation subroutine, there were no errors. Hand calculations were also performed using the Euler method[22] and some of the adjoint variables computed. These matched the values generated by the code. These checks suggest that the code is relatively free of errors. The optimization code took a CPU time of about 1 h 51 min on a DEC 3000 αxp machine (for about 450 iterations).

RESULTS AND DISCUSSIONS

The reference (current operating conditions indicated by "ref") results are first generated using the simulation code[19] for the three initial water concentrations, $[W]_0$, of 3.45%, 2.52%, and 4.43% (by weight). The values of several variables describing the current operating conditions are given by Wajge and coworkers[19] and Sareen and Gupta.[23] These provide values of $conv_d$ and $\mu_{n,d}$ in eqs. (5) and (6), and also provide results against which optimal solutions can be compared. The current (ref) pressure histories for the three values of $[W]_0$ are shown in Figure 2.

Optimal $V_T(t)$ histories are now generated (with $T_j = T_{j,ref}$), using the following parameters:

$$r = 0.1 \qquad (12)$$

$$\epsilon^* = 0.9 \qquad (13)$$

The starting control variable history, V_T^0, is shown in Figure 3 (case 2). This is selected so as to give the starting pressure history shown as Iteration no. 1 in Figure 4. The pressure builds up to a maximum value, $p_{max}(\leq p_{max,ref})$, in the beginning; is then maintained at this value for some period of time; and then decreases slowly to the final value at $t = t_f$ [determined by the stopping condition in eq. (6)]. Figure 4 shows the variation of the pressure history with iteration number during the course of optimization for the $[W]_0 = 3.45\%$ case. The objective function, end-point constraint violation, and the pressure history converge (see Figs. 4–6) to near-optimal values in about 332 iterations. In the initial phase of optimization the convergence is observed to be very rapid, but then it slows down and some oscillatory behavior is observed before final convergence. This kind of oscillatory behavior has been observed in earlier studies[12–14] also. The convergence of the algorithm can be expedited by manipulating the two computational parameters, ϵ^* and r. In the earlier studies[13,14] it has been established that higher values of ϵ^* tend to speed up convergence. But all our at-

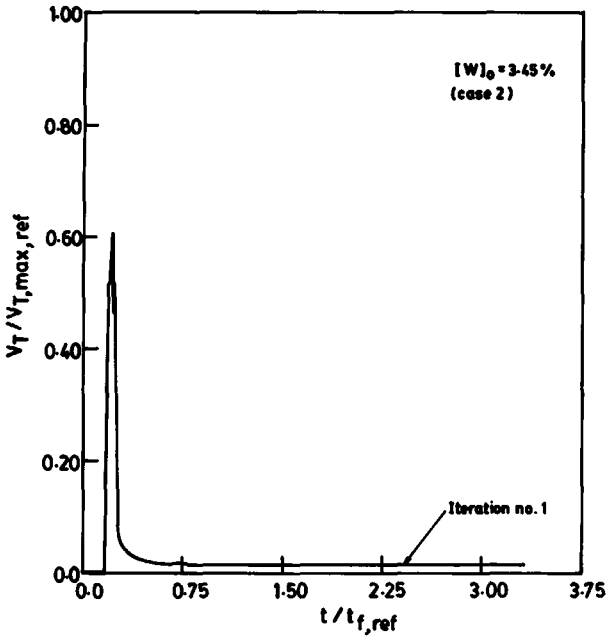

Figure 3 Starting dimensionless vapor release rate history for $[W]_0 = 3.45\%$ (case 2).

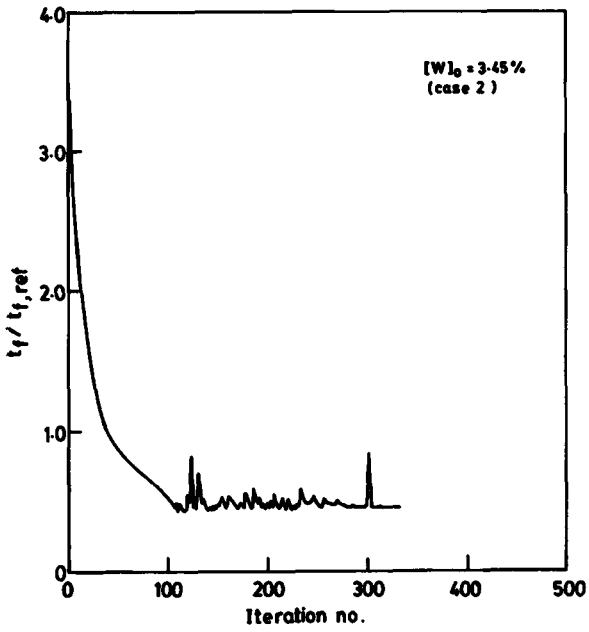

Figure 5 Convergence of objective function, $I\ (\equiv t_f/t_{f,ref})$ with iteration number for case 2 (Fig. 4).

tempts to do so were thwarted by the presence of discontinuities in the model. A large value of ϵ^* results in large values of $\delta\psi_1$, which lead to large changes in the control vector, $V_T(t)$. This results in a sudden drop of pressure. The pressure could go down to such an extent that sudden changes in the interfacial concentrations of monomer and water are observed. The gradient of the monomer concentration (at the bubble surface) then becomes negative. This creates problems in the integration of the state-variable equations, since mass transfer from the bubble to the liquid is not allowed for in the model

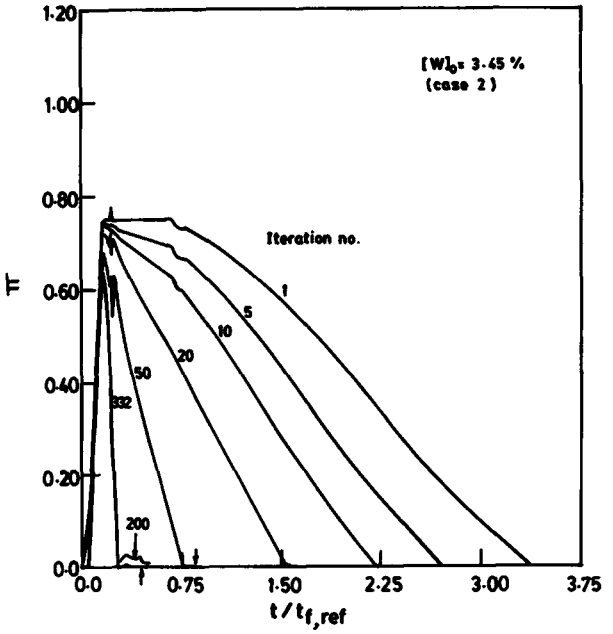

Figure 4 Convergence of dimensionless pressure history with iteration number, for $[W]_0 = 3.45\%$, $\epsilon^* = 0.9$, $r = 0.1$ (case 2).

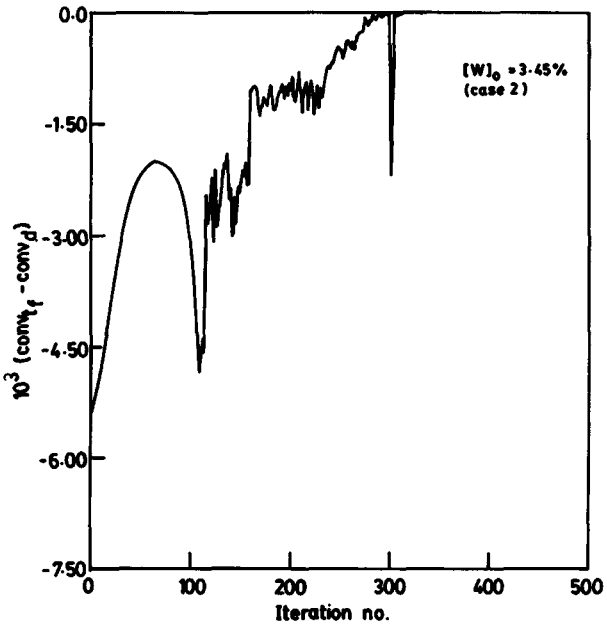

Figure 6 $\psi_1\ (\equiv conv_{t_f} - conv_d)$ versus iteration number for case 2 (Fig. 4).

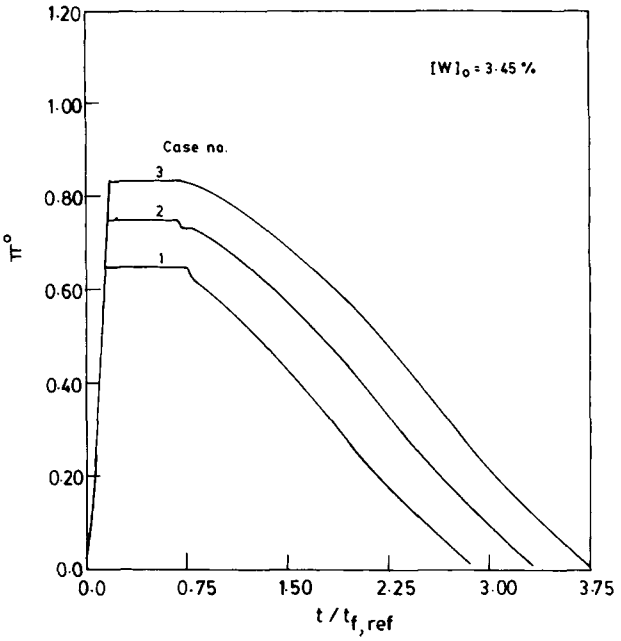

Figure 7 Dimensionless pressure histories corresponding to three different starting V_T histories (cases 1–3).

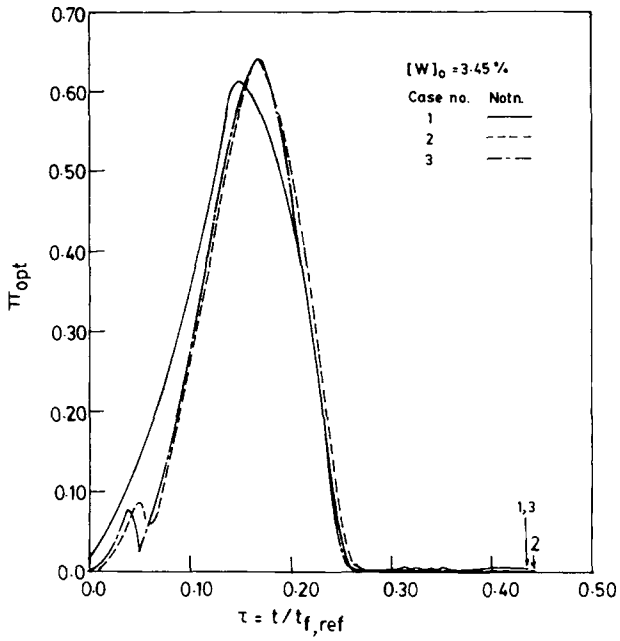

Figure 8 Dimensionless pressure histories for optimal runs corresponding to three different starting V_T histories (cases 1–3).

(and probably does not occur). To avoid such numerical problems, the value of the increment, $\delta V(t)$, is modulated by a factor $\omega(\leq 1)$. In this study the value of ω has been used as 0.75. Therefore, eq. (9) is replaced by

$$V_T^{\text{new}}(t) = V_T^0(t) + \omega \delta V_T(t) \qquad (14)$$

in the algorithm.

One of the most crucial parameters in the control vector optimization technique[17] is the choice of the initial control vector history, $V_T^0(t)$. An improper choice of the initial guess can lead to erroneous results or lack of convergence. A common practice followed in most studies has been to assume a constant value of the control variable at all values of t. In our study, it was not possible to start with such a history since it led to negative gradients of the monomer concentration at the bubble surface. Therefore, a V_T^0 history was selected which corresponded to an initial pressure history, $p^0(t)$, which was somewhat similar to the one currently being used in the industrial reactor (see Fig. 2). Optimization was carried out with three different initial V_T^0 histories (cases 1–3). Figure 7 shows the initial (Iteration no. 1) pressure histories for these three cases. The optimal history is found to be almost independent of the starting history (see Fig. 8), and the values of $t_f/t_{f,\text{ref}}$ (= 0.45) match to two decimal places. Optimization has also been carried out with different combinations of ϵ^* and r. Table II gives the results. It can be inferred that the final results are independent of the values of the computational parameters (provided that the choices are such that negative monomer concentration gradients at the bubble surface are not encountered). It is found that increasing the value of ϵ^* leads to faster convergence (but for certain combinations of the computational parameters, a higher value of ϵ^* leads to erroneous results and oscillatory behavior). Although the value of r does not affect the number of iterations too much, it has some effect on the CPU time and the amount of oscillatory behavior. Higher oscillations result in a sudden rise in the objective function which

Table II Effect of r and ϵ^* on Convergence[a] $[W]_0$ = 3.45% (Case 2)

ϵ^*	r	Iterations	CPU Time (s)
0.75	0.50	374	6734
0.90[b]	0.10	332	6182
0.50	0.05	455	7088
0.50	0.10	455	6628
0.50	0.25	455	7015
0.50	0.50	455	6946
0.50	1.00	455	7023

[a] $t_f/t_{f,\text{ref}}$ = 0.45; $conv_{t_f}/conv_d$ = 1.00 for all cases.
[b] Best value.

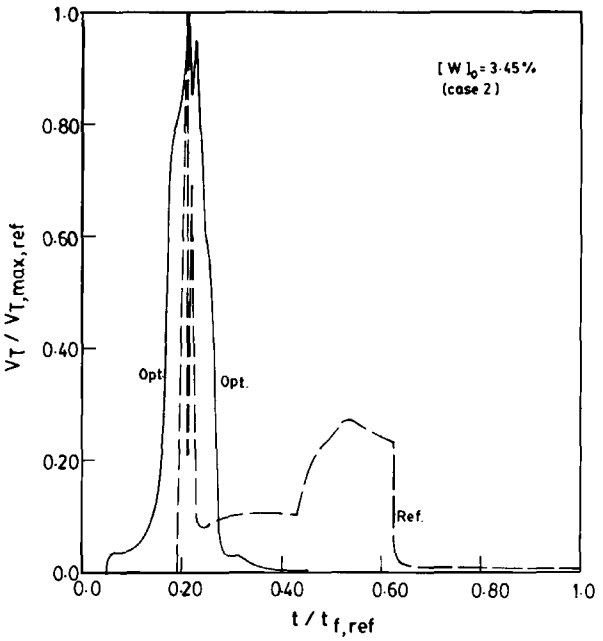

Figure 9 Dimensionless vapor release rate histories. Curve (ref): reference run, (opt): optimal run, for $T_j = T_{j,\text{ref}}$, $[W]_0 = 3.45\%$.

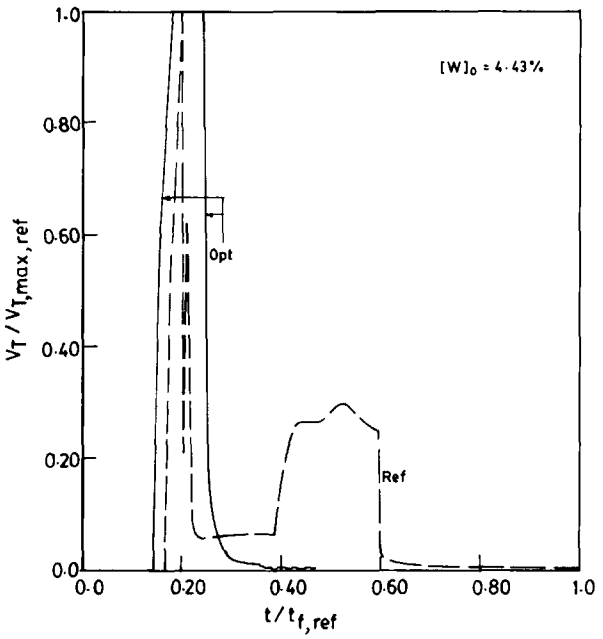

Figure 11 Dimensionless vapor release rate histories. Curve (ref): reference run, (opt): optimal run, for $T_j = T_{j,\text{ref}}$, $[W]_0 = 4.43\%$.

implies a larger number of calculations in the forward and backward integration steps, thereby resulting in higher CPU times. Thus, some amount of numerical experimentation must be performed before the best choices of r and ϵ^* can be deduced. We recommend use of values of 0.9 and 0.1 for ϵ^* and r [eqs. (12) and (13)], respectively, for the present study.

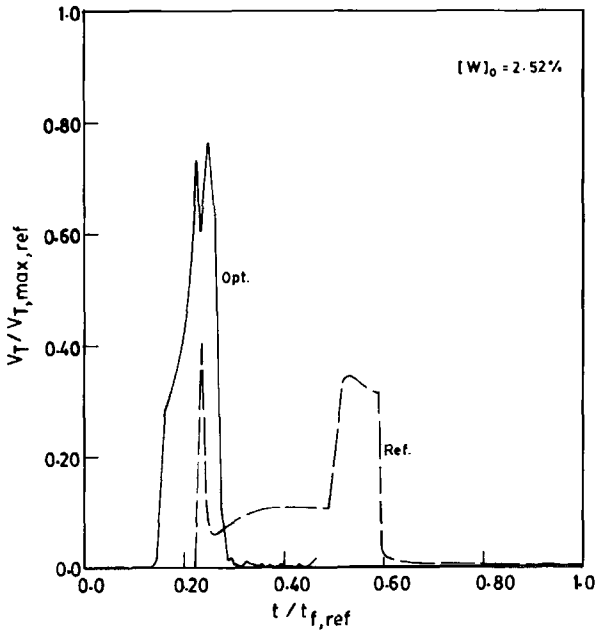

Figure 10 Dimensionless vapor release rate histories. Curve (ref): reference run, (opt): optimal run, for $T_j = T_{j,\text{ref}}$, $[W]_0 = 2.52\%$.

Figure 2 shows the optimal pressure histories (curves marked "opt") for the three values of $[W]_0$. The plot for $[W]_0 = 3.45\%$ is the same as in Figures 4 and 8. The current and optimal vapor release rates are shown in Figures 9–11. Two different maxima in the current V_T histories are observed. The first maximum corresponds to the opening of the valve for the first time to arrest the increase in pressure associated with early vaporization, while the later one is associated with the desired rapid fall of the pressure. It is evident from Figures 9–11 that different pressure histories and vapor release rates are required to produce three different grades of polymer. Table III gives the optimal conditions for the three water concentrations.

Figure 12 shows the variation of μ_n with t for the optimal as well as the reference runs for the three

Table III Optimal Conditions for Three Feed Water Concentrations

$[W]_0$ (%)	$t_f/t_{f,\text{ref}}$	$conv_{t_f}/conv_d$	$[C_2]_{t_f}/[C_2]_{t_f,\text{ref}}$
2.52	0.43125	0.99956	0.2526559
3.45	0.45000	1.00000	0.2584115
4.43	0.46250	0.99977	0.2491274

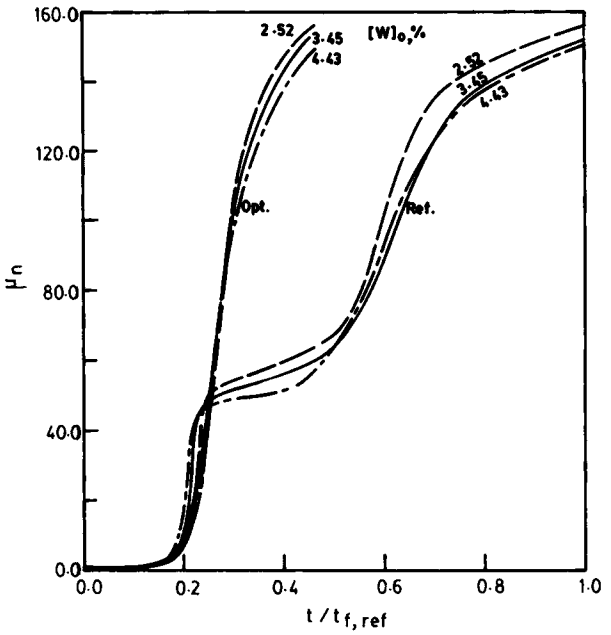

Figure 12 Variation of degree of polymerization with dimensionless time for the reference (ref) and optimal (opt) runs for $T_j = T_{j,\text{ref}}$, $[W]_0 = 2.52\%, 3.45\%, 4.43\%$.

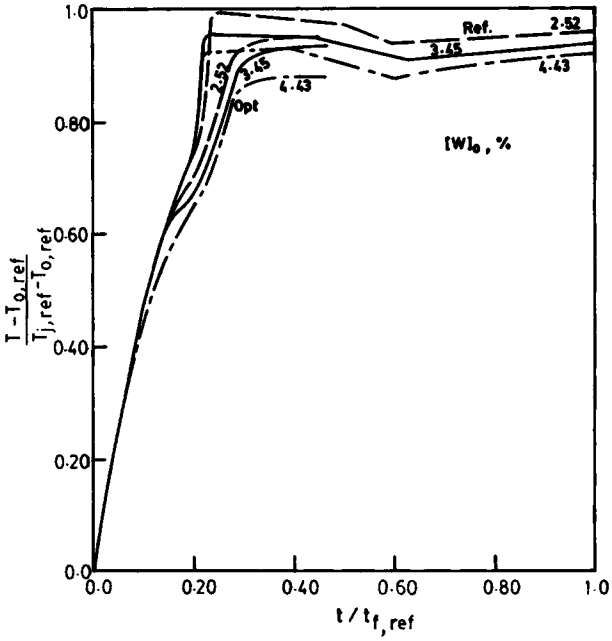

Figure 13 Variation of dimensionless temperature (θ) with dimensionless time for the reference (ref) and optimal (opt) runs for $T_j = T_{j,\text{ref}}$, $[W]_0 = 2.52\%, 3.45\%, 4.43\%$.

$[W]_0$ values. In the reference (current) runs, two distinct regions are observed where μ_n increases, the first being associated with the polyaddition reaction and the second with the polycondensation reaction. There is a short plateau in between the two regimes. From the figure it is evident that this plateau does not exist for the optimal histories because of early and rapid pressure decrease, and the μ_n increases rapidly at an almost-constant rate to the desired value. The value of μ_n approaches its final value almost asymptotically at $t_{f,\text{ref}}$ for the reference runs. This is not so for the optimal runs. This makes it necessary to have an excellent control for the reactor so that the value of μ_n of the product does not exceed the desired value during emptying of the reactor at the end of the run. With the availability of highly sophisticated and robust controllers, this should not pose any major difficulty.

Figure 13 shows the dimensionless temperature histories for the reference runs as well as for the optimal conditions. In the initial phase, when pressure in the reactor is building up, the temperature variations for the reference runs are similar to those for the optimal runs. This is not surprising since the pressure histories for the optimal and reference runs are quite similar (see Fig. 2) in the beginning. However, the temperature histories for the optimal cases deviate from the reference values when the optimal pressure histories start deviating from currently encountered values. This suggests the importance of latent heat effects. Figure 14 shows the variation of monomer conversion with t, for $[W]_0 = 3.45\%$. It is observed that the conversion rises less

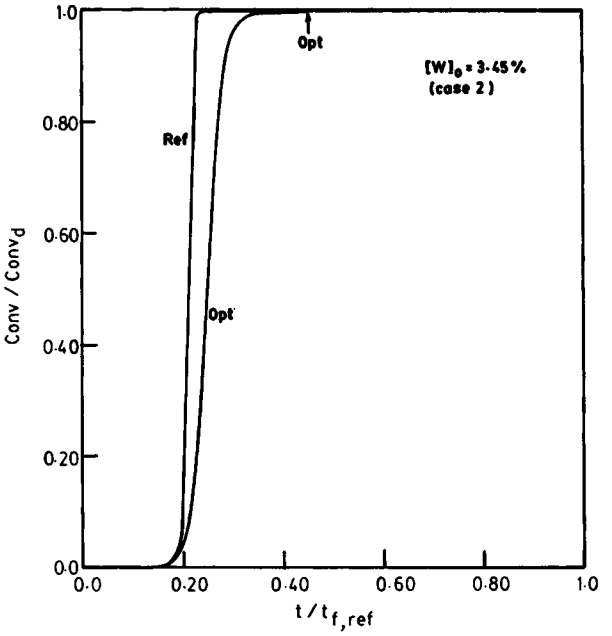

Figure 14 Variation of the dimensionless monomer conversion with dimensionless time for the reference (ref) and optimal (opt) runs for $T_j = T_{j,\text{ref}}$, $[W]_0 = 3.45\%$ (case 2).

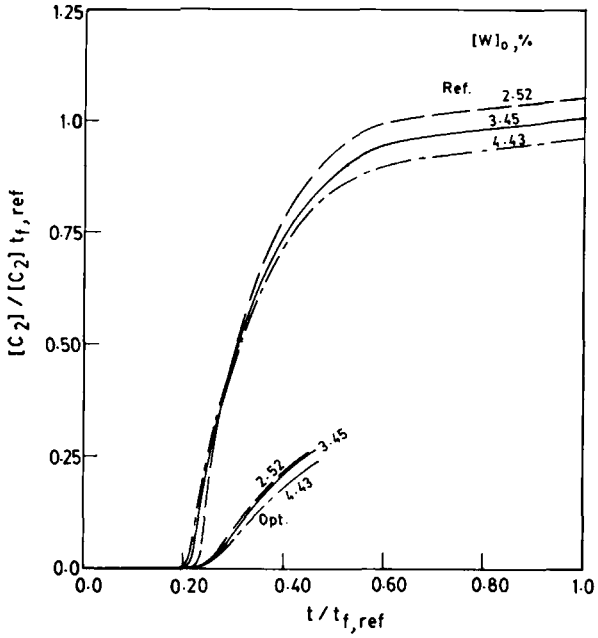

Figure 15 Variation of the dimensionless cyclic dimer concentration with dimensionless time for the reference (ref) and optimal (opt) runs for $T_j = T_{j,\text{ref}}$, $[W]_0 = 2.52\%$, 3.45%, 4.43%.

sharply for the optimal conditions than in the reference case. This is attributed to lower temperatures in the optimal case.

Figure 15 shows the variation of the cyclic dimer concentration, $[C_2]$, with time. The cyclic dimer concentration remains negligible up to some time and then it starts increasing. The final value for the optimal case is found to be considerably lower than the current values. This is a blessing, since we had obtained the optimal $V_T(t)$ without putting any requirements on the cyclic dimer concentrations. It must be kept in mind that the low concentration of $[C_2]_{t_f}$ for optimal runs could increase further during postpolymerization processes (including the emptying of the reactor), since equilibrium is not attained for the reactions involving the cyclic dimer. However, since one would be ensuring that the values of μ_n do not rise beyond the desired values during emptying of the reactor, this requirement should pose no additional problems.

It is interesting to note that the optimal pressure histories obtained (at $T_j = T_{j,\text{ref}}$) in the present study using Pontryagin's minimum principle is quite similar to that obtained by our group earlier,[23,24] in which the *shape* of the pressure history was fixed *a priori*, and was determined completely by a few *constants* ($p_{\max}$, t_c, S, t_f). Optimal values of three of these constants [$p_{\max}$, t_c, and S, with t_f determined by the stopping condition of eq. (6)] were determined using sequential quadratic programming. The similarity of the optimal pressure histories as obtained more rigorously in the present study, with the optimal histories obtained with somewhat artificial constraints put on the *shape* of $p(t)$, confirms the validity of the constraints used in our earlier study. It may be added that major increases in the plant capacity have been achieved using some of the results of the present study.

Figure 16 shows how the optimal pressure history changes when the jacket fluid temperature is increased by 5°C. Higher pressures are required (to suppress the vaporization of monomer and water). Use of higher values of T_j lead to lower values of the objective function. However, it must be ensured that the polymer does not become degraded under these conditions.

In addition to the optimization problem studied above, we also studied the problem (for $[W]_0 = 3.45\%$)

$$\min I[V_T(t),\ T_j = T_{j,\text{ref}}] \equiv t_f/t_{f,\text{ref}} \qquad (15)$$

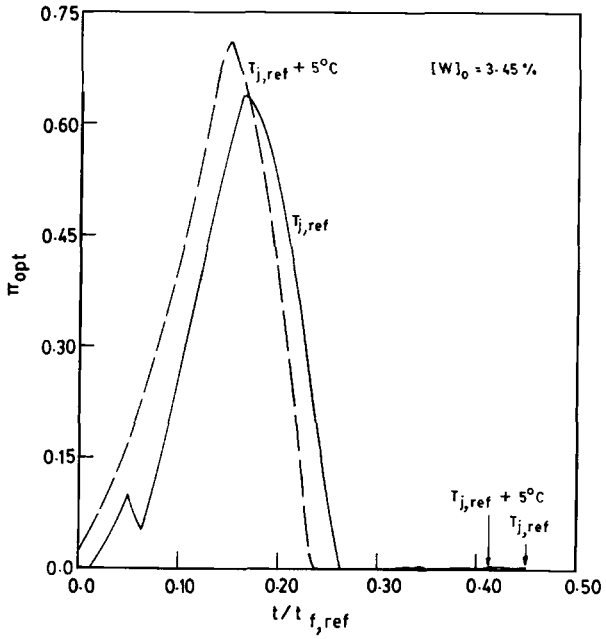

Figure 16 Optimal pressure history using $T_j = T_{j,\text{ref}} + 5°C$ for the $[W]_0 = 3.45\%$ case. Optimal history using $T_j = T_{j,\text{ref}}$ also shown for comparison.

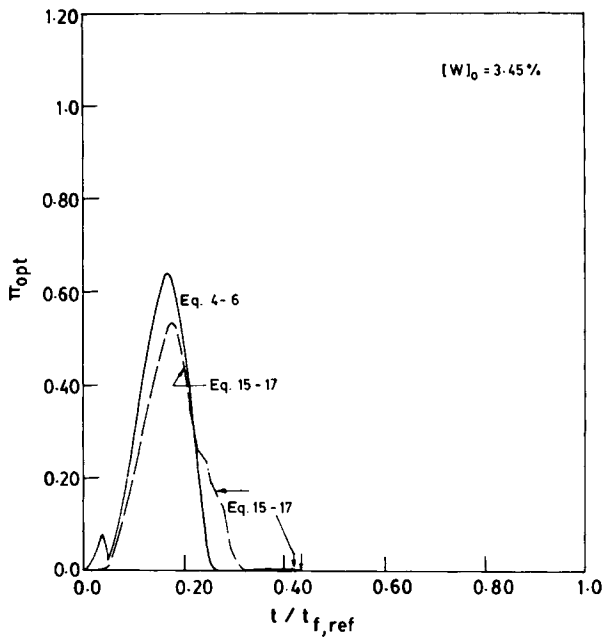

Figure 17 Optimal pressure histories for the two optimization problems described in eqs. (4)–(6) and eqs. (15)–(17) for $[W]_0 = 3.45\%$.

with the end-point constraint/stopping condition

$$[C_2]_{t_f}/[C_2]_{t_f,\text{ref}} = 0.2584115 \tag{16}$$

$$\mu_{n,t_f} = 152 \tag{17}$$

The values of $t_f/t_{f,\text{ref}}$ and $conv_{t_f}/conv_d$ under optimal conditions came out as 0.4375 and 0.96689, respectively, which compare very well with the corresponding values of 0.45 and 1.0000 for the problem described in eqs. (4)–(6). The optimal pressure histories are shown for the two problems in Figure 17. The results for the two problems seem to be in close agreement and indicate that the optimal results are not significantly affected by the type of end-point constraints used.

CONCLUSIONS

Optimal vapor release rate histories for an industrial semi-batch nylon 6 reactor, using Pontryagin's minimum principle, have been obtained. The results predict a significant reduction in the final reaction time while simultaneously (and somewhat fortuitously) leading to fairly low values of the cyclic dimer concentration in the product. These optimal histories can be implemented on the existing reactor without major alterations and investments. The computational skills developed in this work can also be helpful in the solution of more complicated optimization problems, e.g., multiobjective optimization.

This work has been partly funded by a grant from the Research Center, Gujarat State Fertilizer Co. Ltd., Vadodara, India.

NOMENCLATURE

A_i^0, A_i^c	frequency factor for ith reaction in absence (o) and presence (c) of catalytic effect (kg mol^{-1} h^{-1} or kg^2 mol^{-2} h^{-1})
C_i	caprolactam ($i = 1$) and cyclic dimer ($i = 2$)
$conv$	monomer conversion [eq. (7)]
DP	degree of polymerization of polymer product
E_i^0, E_i^c	activation energies for the ith reaction in absence (o) and presence (c) of catalytic effect (J/mol)
F	mass of liquid in reactor at time t (kg)
ΔH_i	enthalpy of the ith reaction (J/mol)
I	objective function
$I_{\psi_1 I}$, $I_{\psi_1\psi_1}$, I_{II}	integrals of modified adjoint variables
k_i	forward rate constant of ith reaction
k_i'	reverse rate constant of ith reaction
K_i	equilibrium constant for ith reaction
n	number of equations for state variables
PDI	polydispersity index
p	pressure (kPa or atm)
$p_{\max}$	maximum pressure (kPa or atm)
r	parameters in optimization code
R	gas constant (J/mol-K)
$R_{V,m}$, $R_{V,w}$	rate of vaporization of monomer (m) and water (w) at time t (mol/h)
S	slope of p versus t curve in our earlier studies[23,24] (atm/h)
ΔS_i	entropy change for the ith reaction (J mol^{-1} K^{-1})
S_n	linear n-mer
t	time (h)
t_f	total reaction time (h)
t_c	time for which $p = p_{\max}$ (h)
T	temperature (K)
T_j	jacket fluid temperature (K)
TOL	tolerance in D02EJF code of NAG library

$\boldsymbol{u}$	vector of control variables, u_i
V_T	rate of vapor release from reactor (mol/h)
W	water
$\boldsymbol{x}$	vector of state variables, x_i

Greek Letters

ϵ^*	parameter in optimization code
μ_k	kth moment of the chain length distribution (k = 1, 2, $\cdots$); $\mu_k \equiv \sum_{n=1}^{\infty} n^k[S_n]$ (mol/kg)
μ_n	number average chain length ($\equiv \mu_1/\mu_0$)
Π	dimensionless pressure [eq. (1)]
τ	dimensionless time [eq. (2)]
θ	dimensionless temperature
ζ_1	total moles of monomer vaporized in reactor until time t (mol)
ω	parameter in eq. (14)
ρ	stopping condition
ψ_1	end-point constraint
λ_i	adjoint variables
$\lambda_i^{I\rho}$, $\lambda_t^{\psi_1\rho}$	modified adjoint variables

Subscripts/Superscripts

d	desired value
f	final (value for the product)
j	Jacket
max	maximum value
o	feed conditions
t_f	value at $t = t_f$
ref	reference (value currently used in industrial reactor)

Symbols

[ ]	concentrations (mol/kg mixture)

REFERENCES

1. H. K. Reimschuessel, *J. Polym. Sci., Macromol. Rev.*, **12,** 65 (1977).
2. S. K. Gupta and A. Kumar, *Chem. Eng. Commun.*, **20,** 1 (1983).
3. S. K. Gupta and A. Kumar, *Reaction Engineering of Step Growth Polymerization,* Plenum Press, New York, 1987.
4. K. Tai and T. Tagawa, *Ind. Eng. Chem. Prod. Res. Dev.*, **22,** 192 (1983).
5. S. K. Gupta and A. Kumar, *J. Macromol. Sci., Rev. Macromol. Chem. Phys.*, **C26,** 183 (1986).
6. P. J. Hoftyzer, J. Hoogschagen, and D. W. van Krevelen, *Proc. 3rd Eur. Symp. Chem. Rxn. Eng.*, Amsterdam, 1964, p. 247.
7. H. K. Reimschuessel and K. Nagasubramanian, *Chem. Eng. Sci.*, **27,** 1119 (1972).
8. K. Nagasubramanian and H. K. Reimschuessel, *J. Appl. Polym. Sci.*, **16,** 929 (1972).
9. W. F. H. Naudin ten Cate, *Proc. Int. Cong. Use of Elec. Comp. in Chem. Eng.*, Paris, 1973.
10. S. Mochizuki and N. Ito, *Chem. Eng. Sci.*, **33,** 1401 (1978).
11. A. Ramgopal, A. Kumar, and S. K. Gupta, *J. Appl. Polym. Sci.*, **28,** 2261 (1983).
12. S. K. Gupta, B. S. Damania, and A. Kumar, *J. Appl. Polym. Sci.*, **29,** 2177 (1984).
13. A. K. Ray and S. K. Gupta, *J. Appl. Polym. Sci.*, **30,** 4529 (1985).
14. A. K. Ray and S. K. Gupta, *Polym. Eng. Sci.*, **26,** 1033 (1986).
15. D. Srivastava and S. K. Gupta, *Polym. Eng. Sci.*, **31,** 596 (1991).
16. R. M. Wajge and S. K. Gupta, *Polym. Eng. Sci.*, **34,** 1161 (1994).
17. W. H. Ray and J. Szekely, *Process Optimization,* Wiley, New York, 1969.
18. M. M. Denn, *Optimization by Variational Methods,* McGraw-Hill, New York, 1969.
19. R. M. Wajge, S. S. Rao, and S. K. Gupta, *Polymer,* **35,** 3722 (1994).
20. L. Lapidus and R. Luus, *Optimal Control of Engineering Processes,* Blaisdell, Waltham, MA, 1967.
21. A. E. Bryson and Y. C. Ho, *Applied Optimal Control,* Blaisdell, Waltham, MA, 1969.
22. S. K. Gupta, *Numerical Methods for Engineers,* New Age International/Wiley Eastern, New Delhi, 1995.
23. R. Sareen and S. K. Gupta, *J. Appl. Polym. Sci.*, **58,** 2357 (1995).
24. R. Sareen, M. R. Kulkarni, and S. K. Gupta, *J. Appl. Polym. Sci.*, **57,** 209 (1995).

Received February 3, 1996
Accepted April 8, 1996